PLOS ONE

RESEARCH ARTICLE

Exogenous α-synuclein hinders synaptic communication in cultured cortical primary rat neurons

G. C. Hassink[1,2☯], C. C. Raiss[3☯], I. M. J. Segers-Nolten[3], R. J. A. van Wezel[2,4], V. Subramaniam[3], J. le Feber[1,2‡*], M. M. A. E. Claessens[1‡]

1 Clinical Neurophysiology, MIRA Institute for Biomedical Technology and Technical Medicine, University of Twente, Postbus, Enschede, the Netherlands, **2** Biomedical Signal and Systems, MIRA Institute for Biomedical Technology and Technical Medicine, University of Twente, Postbus, Enschede, the Netherlands, **3** Nanobiophysics Group, MESA+ Institute for Nanotechnology, University of Twente, Postbus, Enschede, the Netherlands, **4** Biophysics, Donders Institute for Brain, Cognition and Behaviour, Radboud University, Nijmegen, Postbus, The Netherlands

☯ These authors contributed equally to this work.
‡ JIF and MC also contributed equally to this work.
* j.lefeber@utwente.nl

Citation: Hassink GC, Raiss CC, Segers-Nolten IMJ, van Wezel RJA, Subramaniam V, le Feber J, et al. (2018) Exogenous α-synuclein hinders synaptic communication in cultured cortical primary rat neurons. PLoS ONE 13(3): e0193763. https://doi.org/10.1371/journal.pone.0193763

Editor: Philipp J. Kahle, Hertie Institute for Clinical Brain Research and German Center for Neurodegenerative Diseases, GERMANY

Received: July 20, 2017

Accepted: February 17, 2018

Published: March 22, 2018

Data Availability Statement: All relevant data are available from the Dryad repository at the following 10.5061/dryad.m7fk370.

Funding: This project was funded in part from NWO-CW VIDI (https://www.nwo.nl/onderzoek-en-resultaten/programmas/vernieuwingsimpuls/toekenningen/alle+vidi+toekenningen/Toekenningen+Vidi+2009) grant number (700.59.423) to MC and in part by a MIRA voucher (https://www.utwente.nl/mira/) to JIF

Abstract

Amyloid aggregates of the protein α-synuclein (αS) called Lewy Bodies (LB) and Lewy Neurites (LN) are the pathological hallmark of Parkinson's disease (PD) and other synucleinopathies. We have previously shown that high extracellular αS concentrations can be toxic to cells and that neurons take up αS. Here we aimed to get more insight into the toxicity mechanism associated with high extracellular αS concentrations (50–100 μM). High extracellular αS concentrations resulted in a reduction of the firing rate of the neuronal network by disrupting synaptic transmission, while the neuronal ability to fire action potentials was still intact. Furthermore, many cells developed αS deposits larger than 500 nm within five days, but otherwise appeared healthy. Synaptic dysfunction clearly occurred before the establishment of large intracellular deposits and neuronal death, suggesting that an excessive extracellular αS concentration caused synaptic failure and which later possibly contributed to neuronal death.

Introduction

The three most common synucleinopathies are Parkinson's disease (PD), Lewy body dementia (LBD), and multiple system atrophy (MSA) [1]. In all these diseases, the protein α-synuclein (αS) aggregates into amyloid fibrils which are deposited in characteristic inclusions, i.e. Lewy bodies and Lewy neurites [1, 2]. The presence of Lewy bodies does, however, not always correlate with neurodegeneration and disease symptoms [3]. The relation between αS aggregation, the formation of αS amyloid inclusions, clearance of aggregates, and the development of disease remains ill understood.

and MC. The funders had no role in study design, data collection and analysis, decision to publish, or preparation of the manuscript.

Competing interests: The authors have declared that no competing interests exist.

The protein αS is constantly secreted into the extracellular space by αS expressing cells in the brain [4]. More importantly, extracellular αS monomers and aggregates can be taken up by other cells [5–8]. This uptake possibly contributes to spreading of αS aggregation throughout the nervous system [9, 10]. In healthy cells αS function is associated with synaptic activity [11, 12] possibly by regulating the synaptic vesicle pool [13–15] via reclustering of vesicles after endocytosis [16–18]. In αS knockout mice, however, no clear impairment of basic brain functions or neuronal survival could be observed [19]. Therefore Chandra et al hypothesized that αS may have a function in preventing the accumulation of non-native, potentially toxic molecules during the continuous operation of axon terminals [20], like suggested for another abundant protein, cysteine string protein alpha (CSPα) [21, 22].

It is estimated, on the basis of radioactive immuno blots and quantitative mass spectrometry, that the intracellular αS concentration accounts for ~0.5% of total brain protein [14, 23, 24]. With a protein concentration of about 100–200 mg/ml [25], this corresponds to a physiological αS concentration of 35–70 μM in the human brain and ~40μM in the rat brain [26]. For Ubiquitin, cytoskeletal actin, and another Parkinson associated protein, UCH-L1, similar concentrations can be found in the cortex [23, 24, 27]. Mutations in the SNCA gene encoding for αS are directly associated with the development of synucleinopathies and decrease the disease onset [27, 28]. On average, a 1.6 times higher αS concentration is found in neurons of the substantia nigra of elderly people than in young adults as observed by optical densitometry of immune stained tissue slices [29]. A recent post mortem study using western blot showed a fivefold increase in αS concentration in the substantia nigra of brains of MSA patients and a twofold increase in the striatum of MSA and PD patients, as compared to post mortem brains not diagnosed as MSA or PD [30]. Thus, under pathological conditions, local intracellular αS concentrations well above 100 μM are possible, but large differences are found between different cell types and part of the increase can be attributed to presence of αS in inclusion bodies [31]. Much lower concentrations have also been reported in other cell types [32]. Although αS concentrations in cerebrospinal fluid are on average in the nM range (1–300 pg/μl) [33], the extracellular concentration may locally rise much higher, e.g. in case of cell rupture or sudden cell death as a result of mild brain trauma [34, 35]. The extracellular concentration in such cases is unknown, but it may locally increase towards the intracellular concentration. This extracellular αS is possibly removed due to reuptake by glial cells and neurons [36, 37], transport from CSF to the blood serum [38, 39] and degradation by extracellular matrix proteases [40–43]. Earlier work showed that neurons take up excessive αS, leading to the formation of Lewy body like inclusions [37]. The physiological goal of this process remains unclear. Recent work suggests that the formation of LBs occurs simultaneously with synaptic impairment and neuron death, but the exact mechanisms remain unknown [11, 12]. Neuronal uptake of excessive αS has been suggested to be a cellular defense mechanism [44], or to occur as a consequence of the physicochemical conditions in the cell [45], which may in evolutionary perspective be strongly associated. Either way, biology may have found ways to prevent buildup of excessive extracellular αS. Therefore, we hypothesize that temporal excessive extracellular αS might be an initiator of αS related pathology.

We exposed cultured rat cortical networks on multi electrodes arrays (MEAs) to recombinantly expressed human αS (hαS), to investigate the possible detrimental effects of high concentration extracellular αS, e.g. conditions where the extracellular αS concentration approaches the intracellular concentration. Furthermore, we determined if and at what rate LB like inclusions are formed, and investigated the sequence of events that eventually lead to neuronal cell death.

Materials and methods

Recombinant proteins and reagents

The expression of human wild type αS (hαS) and the A140C mutant (hαS 140C) with a single alanine to cysteine substitution at residue 140 was performed in E. coli B121 (DE3) using a pT7 based expression system. Details on the purification procedure of recombinantly produced hαS are described elsewhere [46]. Purified protein was stored at -80˚C in aliquots until further use. The hαS A140C monomers were conjugated with AlexaFluor488 maleimide following the manufacturer's labeling protocol (Life Technologies, USA). Antibodies specific for αS, Amino acids 15–123, 123–140, and 96–140 were obtained from BD biosciences, Abcam, and Santa Cruz Biotechnology, respectively. Rabbit anti-MAP2 antibodies and all Alexa dye coupled secondary antibodies were acquired from Invitrogen.

Aggregation of recombinant hαS

Aggregation of hαS was monitored using the amyloid binding dye Thioflavin T (ThT; excitation: 446nm, emission: 485nm). Fibrilization reactions were set up using 0, 10, 20, 50 and 100 μM αS and 20 μM ThT in R12 medium. The aggregations reactions were performed in 200 μl volume in 96 well plates with optically transparent bottoms, sealed with adhesive film in 6 fold, at 37˚C under quiescent conditions and monitored using a Safire microplate reader (Tecan). The fluorescence intensity was recorded every 15 minutes for 8 days. Before each reading the samples were subjected to five seconds orbital shaking to homogenize the samples. To enable interpretation of intensity values, a control 100 μM sample in 10mM NaCl, 10mM Tris buffer was prepared and allowed to aggregate at 37˚C with orbital shaking. Apart from the orbital shaking the ThT fluorescence intensity of these samples was followed in time under the same experimental conditions. Additionally, pre- and post- ThT incubation samples were loaded on native 4–12 gradient PAGE gels. As a positive control, αS was oligomerized as described elsewere [47].

Atomic force microscopy. Atomic force microscopy (AFM) samples were prepared by adsorbing 10 μl of undiluted R12 medium or undiluted solutions of αS incubated in R12 medium for 8 days on freshly cleaved mica for 4 minutes. These samples were subsequently gently washed twice with 100 μl Milli-Q water and dried using a gentle stream of nitrogen gas. AFM images were acquired on a Bioscope Catalyst (Bruker) in tapping mode in air using a silicon probe (NSC36, tip B; Mikromasch). All images were captured with 512x512 pixels at a scan rate of 0.5 or 2.0 Hz. The images were plane corrected using Scanning Probe Image Processor (SPIP)-6.0.13 software (Image Metrology).

ANS binding assay. To detect and characterize partially folded oligomeric αS species [48] a 200 μM 1-anilinonaphthalene- 8-sulfonic acid (1,8-ANS) stock solution in methanol was prepared. From the aggregation reactions 50 μl aliquots were diluted to 2 ml in 10 mM Tris-HCl, pH 7.4 and 40 μl of 1,8-ANS stock solution was added. As a reference sample 40 μl of 1,8-ANS stock solution was added to 2 ml of 10 mM Tris-HCl, pH 7.4. Fluorescence emission spectra were recorded on a Cary Eclipse fluorescence spectrophotometer (Varian) with excitation at 395 nm and emission detection from 410 to 600 nm using 5 nm slit widths.

Primary neuron extraction and culture

The extraction and culturing of primary neurons was performed as described elsewhere [49]. In short, cells were obtained from newborn Wistar rats from an in-house breeding program using rats obtained from Harlan, Horst, the Netherlands. Rats were decapitated with no prior anesthesia, cortices were isolated, and cells were dissociated by trypsinization and trituration

and subsequently cells were plated on polyethyleneimine (PEI; Acros Organics, USA)-coated culture dishes with glass bottoms or PEI-coated coverslips to ~60% density. After 2 hours, adhered cells were washed with Dulbecco's Modified Eagles Mediun (DMEM; Invitrogen, USA) and cultured in 900 μl, serum-free R12 medium [50] at 37˚C with 5% CO_2. Medium was refreshed twice a week by replacing one third of the medium by the same amount of fresh medium. After three weeks cultures were mostly confluent, and were considered mature.

For electrophysiological experiments, cells were plated on multi electrode arrays (MEA; Multi Channel Systems, Reutlingen, Germany), containing 60 titanium nitride electrodes (30 μm diameter and 200 μm pitch). Cells were plated on MEAs at a final density of approximately 2500 cells/mm^2. For experiments 50 or 100 μM αS was added to mature neural networks. As a control the small stable moderately non-reactive protein bovine serum albumin (BSA; Sigma-Aldrich; 100 μM) was used. For electrophysiological recordings, we firmly sealed the culture chambers with watertight but CO_2 and O_2 permeable foil (MCS; ALA scientific), and placed the cultures in a measurement setup outside the incubator while maintaining temperature, pCO_2, and humidity. Experiments lasted five to seven days. During experiments the culture medium was refreshed once, after four days. Fresh medium did not contain new αS or BSA. All experiments were done at least 20 days after plating. Recordings began after an accommodation period of 20 minutes. All procedures involving animals were conducted according to Dutch and European laws and guidelines, and approved by the Dutch Animal Use Committee (DEC).

Immunocytochemistry

Cell samples were washed with PBS and fixed in 3.7% paraformaldehyde/PBS solution. For immunolabeling, cells were permeabilized with 0.3% Triton X-100 and 0.1% BSA in PBS. Autofluorescence was quenched with 50 mM NH_4Cl in PBS. Primary antibodies were applied in 16% goat serum, 0.3% Triton X-100, 0.3 M NaCl in PBS, and incubated overnight. Subsequently, cells were washed three times with 0.3% Triton X-100 and 0.1% BSA in PBS at room temperature. Secondary antibodies were applied in same buffer and incubated for one hour. For ThioflavinS (ThS) or phalloidinalexa647 staining, fixed cells were incubated with 0.05% ThS or 70 nM phalloidinalexa647 in PBS for 15 minutes. Nuclear counterstaining was performed by incubation in 300 nM 4',6-diamidino-2-phenylindole (DAPI) in PBS for 10 minutes. After washing with PBS, samples were mounted with mounting medium (Ibidi, Germany).

Confocal microscopy

Confocal laser scanning microscopy images were obtained on a Zeiss LSM510 Confocal microscope with a 63x oil immersion objective (NA = 1.4, Zeiss, Germany). Images were taken successively, and were analyzed with the ZEN software 2009 (Zeiss, Germany).

Quantifying the number of αS deposits

To quantify the number of αS deposits, images of three random regions (150 x 150 μm) of samples immunolabeled for αS were obtained at different time points with confocal microscopy. The fluorescence intensity from the αS deposits is typically very high. In the image analysis procedure we therefore set a threshold above which only αS deposits were visible. The same threshold was applied to all images. The αS deposits and cells (DAPI) per image were counted and averaged.

Immunoblot analysis

Cells were incubated in buffer [4x Laemmli buffer (8% SDS, 240 mM Tris-Cl, pH 6.8), 100 mM DTT] for 15 minutes at room temperature and transferred to Eppendorf tubes. The samples were boiled for five minutes and centrifuged for two minutes at 12000 rcf (IEC Micro-MAX tabletop centrifuge). Subsequently, the proteins in the samples were separated on a 12% SDS-PAGE gel. The resulting gel was imaged (excitation.: 488 nm, emission.: 510–600 nm) on a gel imaging system (Gel DocTM, Bio-Rad, USA).

Metabolic activity assay/ live dead assay

Cells seeded in 24-well plates (Greiner Bio-One GmbH, Germany) were incubated with 100 μM hαS monomers or 100 μM rotenone for one, five, or seven days. Rotenone was used as positive control for toxicity. Cells were incubated with 0.5 mg/ml 3-(4,5-dimethylthiazol-2-yl)-2,5-diphenyltetrazolium bromide (MTT) in medium for four hours at 37˚C in an atmosphere containing 5% CO_2. The medium was discarded carefully and cells were solubilized in DMSO. After cell solubilization, the metabolic activity was quantified in a multiwell plate reader by measuring the absorbance at 540 nm (Tecan Ltd, Switzerland). The background absorbance was determined at 690 nm and subtracted from the MTT signal. The MTT data of treated groups were normalized to a control at the same time point. In short, cells were plated on glass cover slips, washed with cold PBS and incubated with 100 μl/ml solution of propidium iodide (PI) and/or annexin V (Invitrogen, USA) for 15 minutes at room temperature. Subsequently, cells were washed with binding buffer. Images were obtained using an inverted fluorescence microscope (EVOS, AMG, USA) with a 20x objective (N.A. = 0.4, EVOS, USA).

Activity recording and wave shape analysis

Action potentials (spikes) on MEAs were measured extracellularly, generally with a negative potential [51]. We calculated the array wide firing rate (AWFR) as the summed activity of all electrodes in one hour time bins. In continuous recordings, 12 consecutive bins were averaged to monitor AWFR at a temporal resolution of two samples/day. In discontinuous recordings (particularly control experiments with BSA), all one hour bins with an AWFR value that fell within a 48h interval were averaged per culture, and then averaged across cultures. AWFR generally increases during the first three weeks after plating. After that, from week three to week seven, predominantly minor fluctuations are observed and a fairly stable mean firing rate on a time scale of hours to days can be observed [52]. Firing patterns usually contained periods of seemingly uncorrelated firing, alternated by periods of highly synchronized firing at many electrodes (network bursts). Data were recorded from all electrodes at a sample rate of 16 kHz, using a custom Labview (National Instruments, Austin (Tx), USA) program. Potential spikes were stored whenever the signal exceeded a predefined threshold of 5.5 times the estimated noise level (which was continuously updated). For each spike, the program stored the time stamp, the recording electrode and 6 ms of the spike waveform (from 2 ms before to 4 ms after the threshold crossing).

Stored wave shapes were used for off-line artifact detection following the procedure described in [53]. If αS affects neuronal viability, or, more generally, the resting membrane potential [54], this is also reflected in a change in the action potential, which can be detected in extracellular potential recordings [55]. In MEA recordings, electrodes may pick up signals from more than one neuron. For this analysis, however, we selected electrodes that recorded activity from a single neuron, following the approach introduced in [56]. In short, a measure is calculated for the variability of action potential shapes at each electrode. Electrodes with sufficiently low variability during baseline were considered as single neuron electrodes. Wave

shapes were averaged per electrode in 1 h time bins. In each bin we calculated the relative amplitude (normalized to baseline) and the correlation coefficient between the action potential shape of that hour and those of all preceding hours. All activity of individual cultures was normalized to the baseline activity before averaging across cultures. Finally, for each neuron, the time of last activity was determined. Neurons with a correlation coefficient of more than 0.9 and a relative amplitude of more than 0.75 at the time of last activity, were considered to have unchanged action potential shapes.

In addition to spontaneous activity recordings, some cultures were electrically stimulated during 25 minutes per two hours. In these experiments, all data recorded from the start of the stimulation period until 10 minutes after this period were excluded for the analysis of spontaneous activity, wave shape, and synchronicity (see below).

Burst synchronization analysis

Synchronized network bursts depend on synaptic transmission, and as such provide a suitable indicator of synaptic functioning. To analyze the relative occurrence of network bursts we determined a burstiness index (BI) [57]. In short, five minute recordings were divided into 300 (1s) time bins and the total number of spikes in each bin, summed across all electrodes, was counted. The number of spikes in the 45 bins (15% of all bins within the 300 s period) containing the largest spike counts (f15) was expressed as a fraction of the total amount of spikes in that 300 s period. Should most of the spikes occur in bursts, f15 will be close to 1; tonic firing should lead to f15 $\approx$ 0.15. We then defined a BI such that BI = (f15-0.15)/0.85, such that BI is normalized between 0 (no bursts) and 1 (burst dominated). Five minute periods with less than 600 spikes were excluded from this analysis.

Stimulation experiments

Diminishing neural activity after αS addition may reflect decreased neuronal excitability or impeded synaptic transmission. To differentiate between these two possible causes of reduced activity, cultures were electrically stimulated (bi-phasic square pulses, 200 μs per phase, 16–32 μA, one stimulus pulse per 10 seconds during 25 minutes per two hours). [58]. Electrical stimulation has been shown to induce a response in two phases. The first phase results predominantly from direct stimulation of neurons in the near proximity of the stimulating electrode and (antidromic) activation of axons in this area [59, 60]. The second phase, called network or synaptically mediated response, results from synaptically propagated signals neurons that fired in the first phase to connected neurons, thus creating a wave of activity throughout the network. The first phase (early response) is relatively fast, it typically terminates within 5–15 ms, and besides directly induced action potentials it may contain some synaptically induced spikes [61]. The synaptically mediated response, typically 15–300 ms after the stimulus, can be completely abolished by Glutamatergic receptor antagonists (2R)-amino-5-phosphonovaleric acid (APV) and 6-cyano-7-nitroquinoxaline-2,3-dione (CNQX) [62]. All cultures were stimulated using three pre-selected electrodes that were able to trigger a good network response. The lowest amplitude that was able to induce a network response was determined, usually in the range of 16–32 μA. The stimulation protocol consisted of pseudo random stimulation of the three selected electrodes at 10 seconds intervals. Each electrode was stimulated 50 times, resulting in a total stimulation period of 25 minutes. The stimulation period was repeated every two hours. Only stimulation electrodes that showed an averaged, (combined direct and late) response of at least 60 action potentials per stimulation during baseline measurements were included in this analysis.

Results

Recombinant hαS does not aggregate into amyloid fibrils in medium

After eight days of incubation of hαS in medium the ThT fluorescence intensity of this solution was comparable to the ThT intensity observed for the buffer control sample. Moreover, the ThT intensity did not increase with increasing hαS concentration (Fig 1A). The ThT intensity of medium containing hαS was two orders of magnitude lower than that of control samples containing αS amyloid fibrils, suggesting that no amyloid fibrils were formed. The absence of amyloid fibrils in medium was confirmed in AFM images. However, the images show small structures with a height of approximately 10 nm (Fig 1C). Although this height agrees with the diameter observed for αS oligomers [47, 63], similar structures are found for R12 medium deposited on mica (Fig 1D). We did not observe any difference in ANS fluorescence between R12 medium with or without 100 μM αS (Fig 1B). Western blots of hαS in R12 medium, made after five days of incubation, showed very low amounts of oligomeric αS (Fig 1E). Control blots indicated that these oligomeric species were already present before R12 incubation. We therefore conclude that in the experimental time frame no fibrils are formed but the solution does contain small amounts of oligomeric αS species.

Primary neurons contain endogenous αS and take up extracellular αS

We tested eight neuronal cultures for expression of rat αS (rαS) by immunoblot analysis at different time points. Two weeks after plating we observed expression of rαS. The molecular weight of the endogenous rαS is comparable to that of recombinant expressed human αS (hαS). After three weeks we observed increased expression of both endogenous rαS and the neuron specific marker MAP2, while the expression of the housekeeping enzyme GAPDH

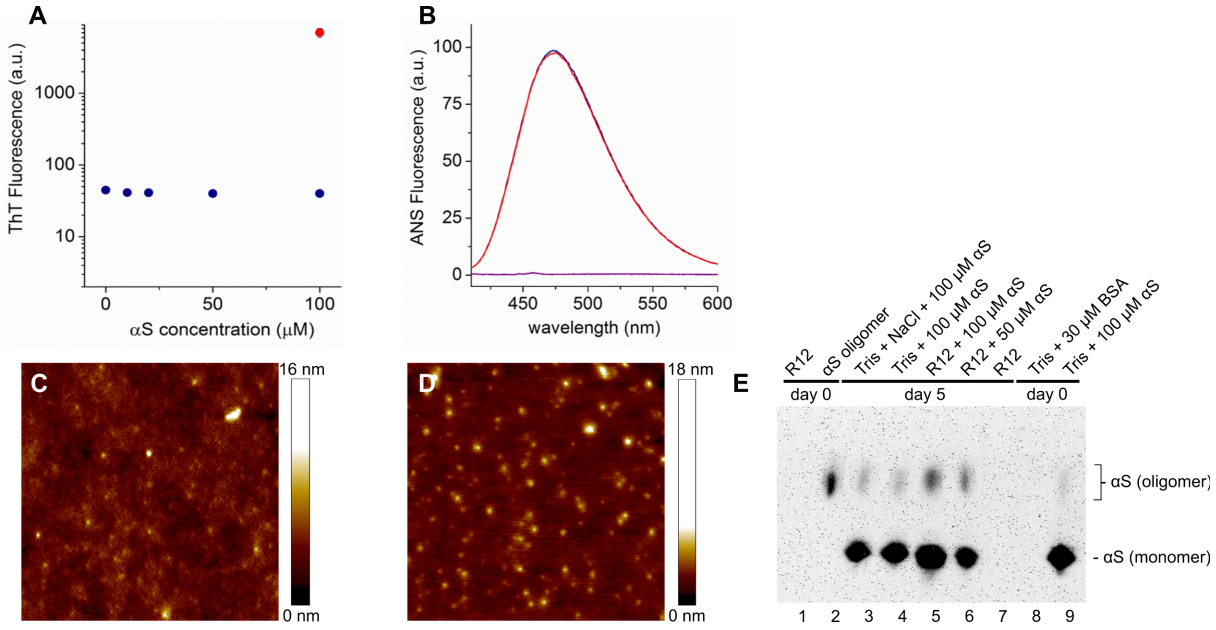

Fig 1. hαS does not aggregate into amyloid fibrils in R12 medium. A) Fluorescence intensity of the amyloid binding dye ThT as a function of the hαS concentration after incubation in R12 medium for eight days at 37˚C (blue) and hαS fibril control sample (red). B) Fluorescence spectra of 1,8-ANS incubated in R12 medium for eight days at 37˚C in the presence of 100 μM hαS (red) and without hαS (blue). As a reference the fluorescence spectrum of 1,8-ANS in 10 mM Tris-HCl, pH 7.4 is shown (purple). C) Representative atomic force microscopy (AFM) height image of a 50 μM hαS sample after eight days of incubation in R12 medium indicating that the samples contained small structures. D) In AFM images of the deposited R12 medium with no added hαS similar structures were found as those observed in C). E) Native western blot showing hαS after incubation in 10mM Tris buffer or R12 medium for 0 and 5 days at 37˚C.

https://doi.org/10.1371/journal.pone.0193763.g001

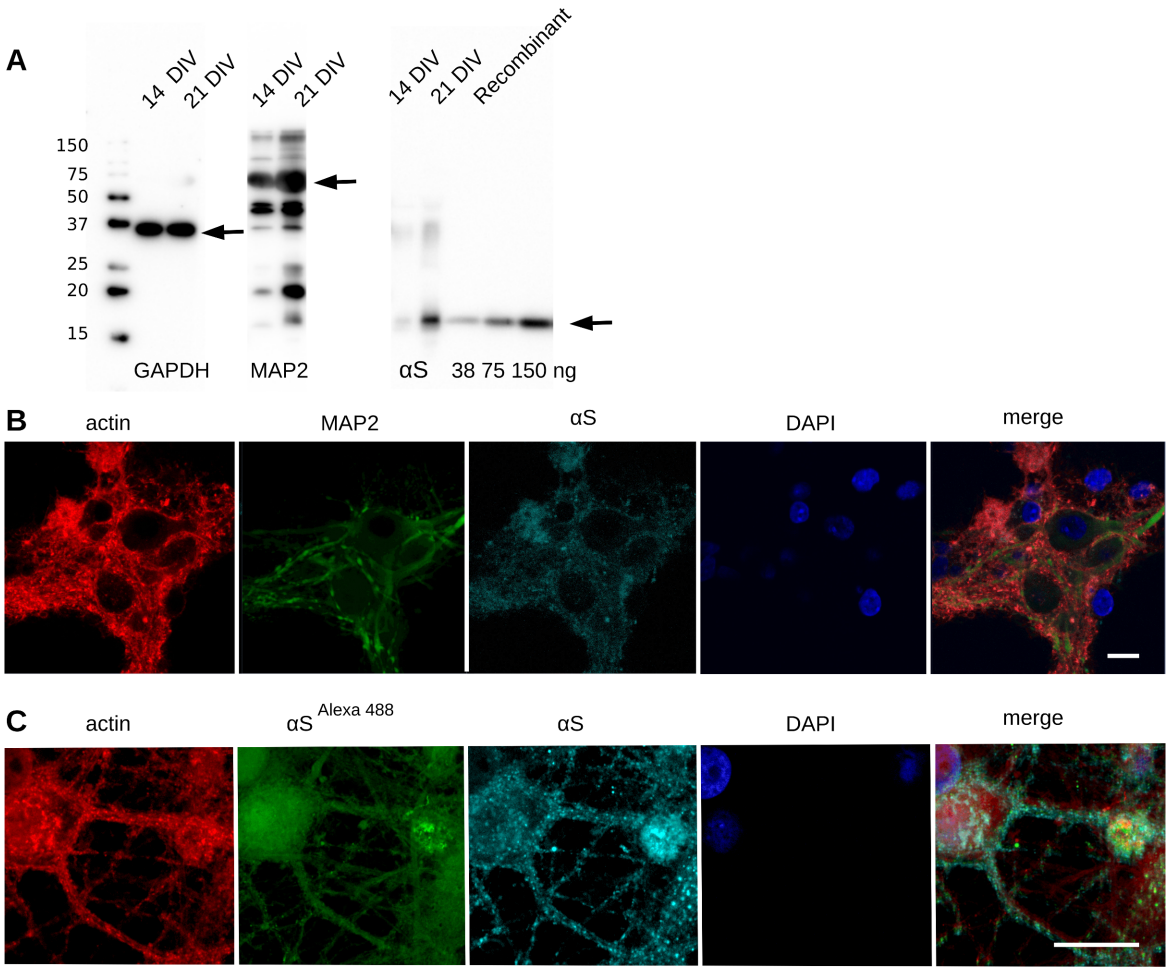

Fig 2. Primary neuronal cells express endogenous rαS and neuronal marker MAP2. A) Immunoblot of cell lysate of primary neuronal cells after 14 days shows immuno-reactivity for MAP2 and αS. B) Cells were fixed and fluorescently labeled; red: phalloidin ^{alexa647}, cyan: αS ^{alexa594}, green: anti-MAP2 ^{alexa488}, blue: DAPI; confocal microscopy; scale bar 10 μm. C) Cells were treated with 100 μM labeled hαS ^{alexa488} and unlabeled hαS monomers (ratio 1:3) for six hours and processed as in B; red: phalloidin ^{alexa647}, green: exogenous hαS ^{alexa488}, cyan: anti-αS ^{alexa594} (endogenous rαS and exogenous hαS), blue: DAPI; confocal microscopy; scale bar 5 μm.

https://doi.org/10.1371/journal.pone.0193763.g002

stayed constant (Fig 2A), indicating that neurons matured during that time. Quantification of the rαS expression using the blot and taking recombinant hαS as a standard (Fig 2A **lanes 8–10**) resulted in an estimate for the total concentration of rαS of 20–50 μM αS at 21 days in vitro (DIV). This is comparable to the rαS concentration in rats reported by others [26]. Immunostaining of the cells showed that rαS was expressed only in MAP2 positive neurons/cells (Fig 2B) and homogeneously distributed throughout the cell.

To visualize the uptake of extracellular hαS, fluorescently labeled monomeric hαS (hαS alexa488) was added to the culture medium. With confocal microscopy, we observed significant uptake of hαS alexaA488 by cells within six hours after addition, in both cytoplasm and nucleus (Fig 2C).

Exogenously added hαS hardly affects cell viability and metabolic activity

Increased amounts of endogenous αS can be toxic to cells [11, 64–72]. To investigate whether this also applies to exogenously added hαS, we evaluated the cytotoxic effect of externally

applied hαS on the cultures of primary rat neurons. Exposure to hαS did not affect cell substrate adhesion as we did not observe increased cell detachment, compared to the control group (data not shown). Neither the live-dead marker, propidium iodide, nor the apoptotic marker Annexin V, showed a significant increase in positive cells for hαS exposed samples compared to control cells (hαS 1.3 ± 1.4% compared to control 1.8 ± 2.0%, P = 0.34 (t-test) and hαS 7.2 ± 7.2% compared to control 3.8 ± 3.4%, P = 0.51, respectively) after seven days of treatment.

Since we did not detect an effect on cell viability, we next evaluated whether exogenously added hαS has an effect on the metabolic activity as measured in a MTT assay. Metabolic rates tended to increase immediately after exposure to hαS to 131.6 ± 8.4%, compared to control samples (P = 0.25; t-test). After seven days metabolic rates had returned to control values (102.1 ±7.7%). In the presence of rotenone, a significant decrease of metabolic activity was observed after addition (47.2 ±2.0%; data not shown in Figure).

Exogenous hαS promotes intracellular αS deposit formation

To assess if the high extracellular hαS concentration induced the formation of αS deposits, cells treated with hαS were immunolabeled for αS and analyzed by confocal microscopy. Fig 3A shows that αS deposits larger than 500 nm were formed within seven days. Occasionally deposits were also actin positive, indicating their intracellular location, as visible in Fig 3A, middle white arrow. A more detailed characterization of αS deposits can be found in Raiss et al. 2016 (Sci Rep). The number of αS deposits increased in time (Fig 3B–3H). Whereas only

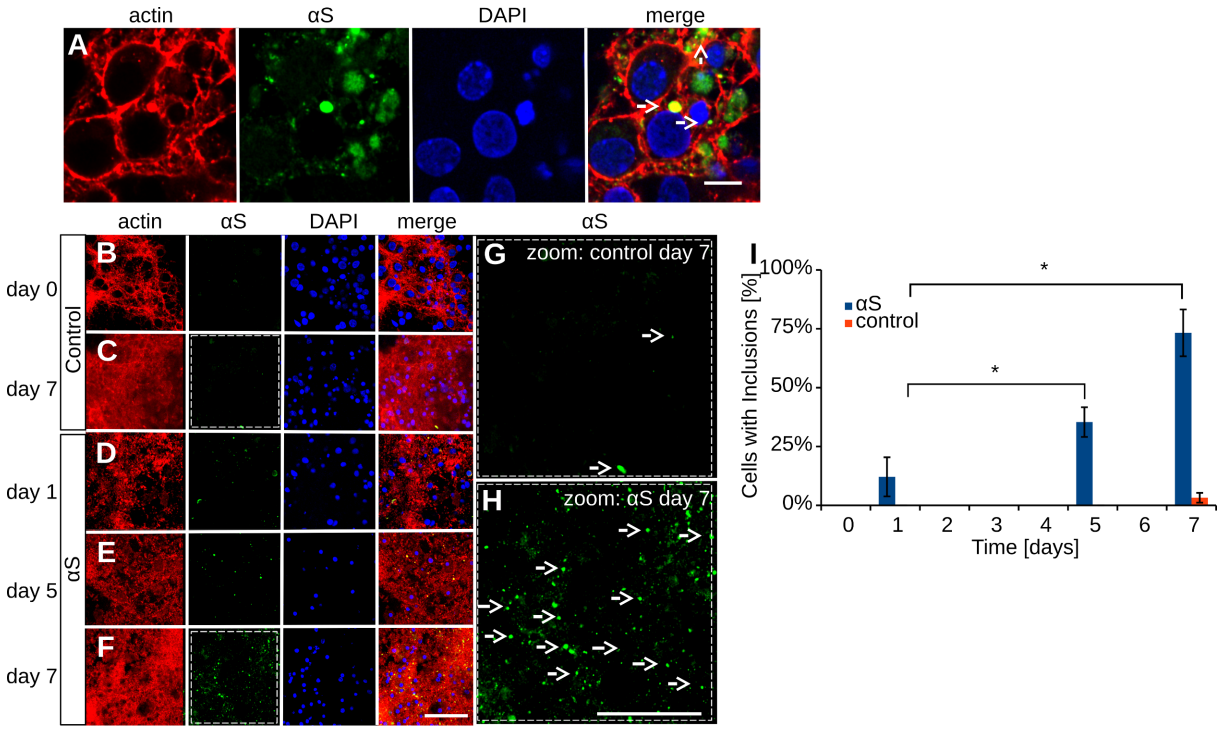

Fig 3. Exogenous hαS induces αS deposit formation in primary cortical cells. Cultured cortical cells were exposed to 100 μM hαS monomers for one, five and seven days. Cells were fluorescently labeled with actin^{phalloidin647}: red and anti-αS ^{alexa594}: green; confocal microscopy; A) After hαS exposure, αS deposits were observed in the cells. Note the actin positive staining of deposit (middle arrow), confirming the intracellular location. B-C) αS deposits formed in control cells. D-F) αS deposits formed in cells exposed to exogenous hαS. G-H) Magnification of αS immunolabeled cell cultures at day seven. I) The number of αS deposits per cell; n = 3 for all groups; paired student's t-test: * indicates P<0.05; scale bar 5 μm (A), 50 μm (B-F) and 10 μm (G-H); αS deposits are indicated by white arrows.

https://doi.org/10.1371/journal.pone.0193763.g003

few αS deposits were found after one day of αS exposure, about a third of the cells contained an αS deposit by day five, and 75% of all cells contained a deposit by day seven (Fig 3I).

Exogenous hαS alters neuronal activity and burst synchronization but leaves the action potential amplitude and shape unchanged

In eight cultures, we recorded electrophysiological activity, and we investigated the effect of the added recombinant hαS. Initially, all cultures were active (9.9 ± 2.3 (SEM) spikes per second) and their activity patterns included periods of highly synchronized action potential firing, i.e. all cultures regularly showed network bursts. The array wide firing rate showed an initial increase, directly after administration of hαS, which lasted from a few hours up to a full day. The magnitude of the increase varied per experiment as reflected by the relatively large error bars (Fig 4D). After the initial increase, the AWFR decreased and dropped below baseline values within approximately 24 hours. The firing rate decreased significantly until day five, when hardly any activity could be recorded (one-way ANOVA: $p<0.01$, Fig 4D and compare Fig 4A and 4B). Whereas initially action potentials were recorded at most electrodes, with time an increasing number of electrodes became silent particularly beyond day three ($p<0.001$, Fig 4C). The burstiness index remained stable for the first two days and then decreased significantly ($p<0.001$, (Fig 4E). After five days the activity was too low to calculate the burstiness index. In four control cultures treated with 100 μM BSA, only the number of active electrodes decreased with time (one-way ANOVA: $p<0.02$), but to a significantly lesser extent than in hαS treated cultures (two-way ANOVA: $p<0.05$). AWFR and burstiness were not significantly affected ($p = 0.18$ and $p = 0.29$, respectively, Fig 4C and 4E).

We next analyzed the temporal development of the shapes of the action potentials, at those electrodes that recorded single unit activity. Each presented action potential is the average of all action potentials recorded at a particular electrode within a one-hour period. Superposition of all resulting averaged action potentials of a representative electrode clearly shows that shape and amplitude of the averaged action potential remained constant throughout the experiment (Fig 4F). This constant shape of the action potential over time was observed at the majority of the selected electrodes. Fig 4H shows that a significant portion (60%) of neurons had unchanged action potential shapes when they stopped firing. (Fig 4G and 4H). In contrast to the 100% silencing observed in αS treated cultures, only 50% of the neurons had stopped firing after eight days in cultures treated with BSA. Of those neurons only 5% showed unchanged action potentials. Remarkably, most action potential shapes, if changed at all, did not change gradually over time, but rather suddenly during the last hours before they stopped firing, as shown in Fig 4G **right panel**.

Synaptic transmission is hampered in hαS exposed neurons

To assess the quality of synaptic transmission, early (5–15 ms latencies) and late responses (15–300 ms) to electrical stimulation were measured and normalized to baseline responses (before the addition of hαS, Fig 5A). Late responses started to decrease almost directly after hαS administration whereas early responses remained around baseline for two days. The late response continuously decreased for four days until we were no longer able to measure any late responses (Fig 5B). A similar temporal evolution was observed when αS was administered at 50μM for both late response (two-way ANOVA: $p = 0.17$ Fig 5B) and AWFR (two-way ANOVA: $p = 0.28$ **Figs** 5C **and** 4D). Two control cultures treated with BSA were electrically stimulated, late responses remained above 80% of their baseline response for at least 40 and 100 hrs, respectively, after which the recordings were stopped (data not shown).

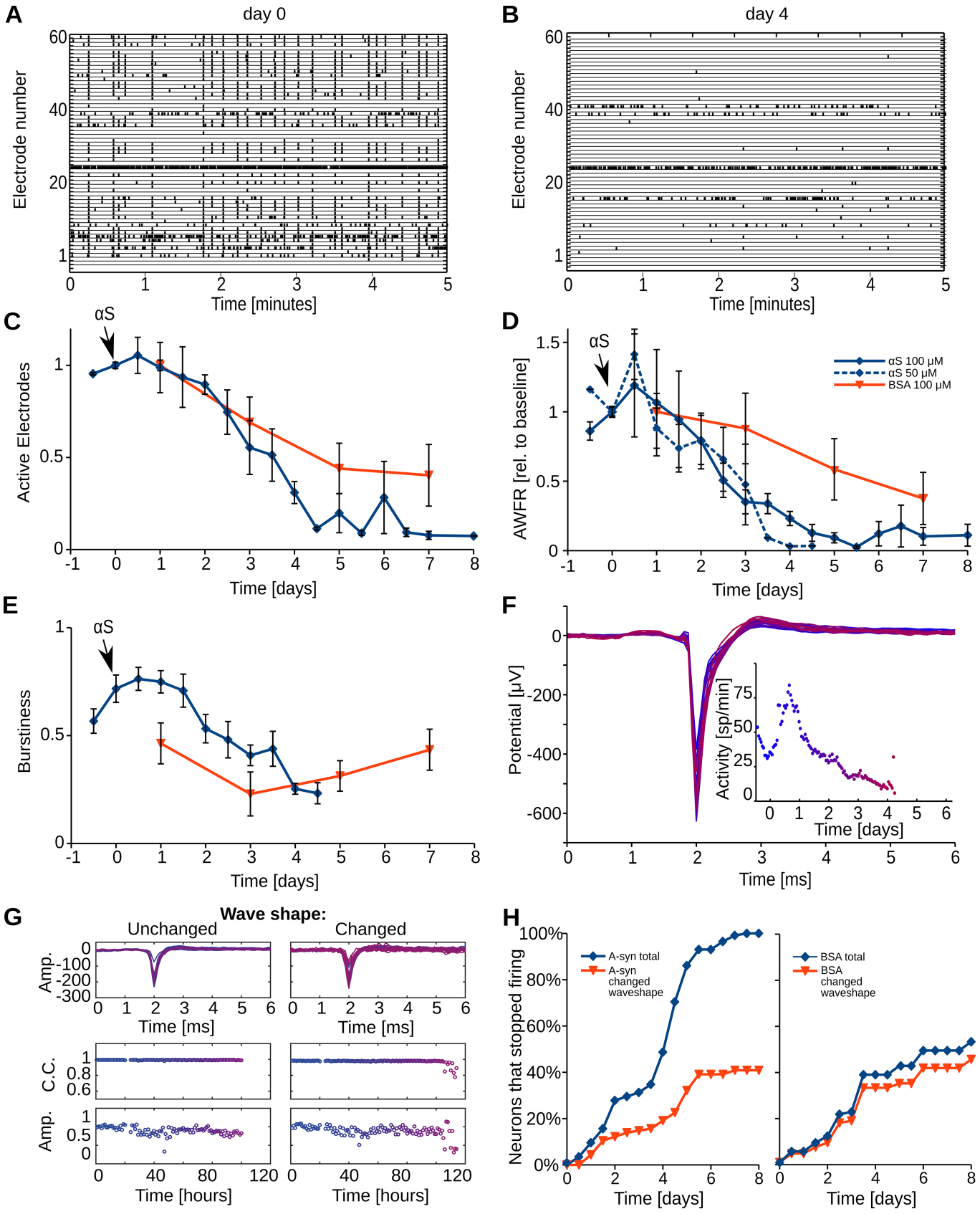
A
day 0
Electrode number
Time [minutes]
B
day 4
Electrode number
Time [minutes]
C
αS
Active Electrodes
Time [days]
D
αS
αS 100 µM
αS 50 µM
BSA 100 µM
AWFR [rel. to baseline]
Time [days]
E
αS
Burstiness
Time [days]
F
Potential [µV]
Activity [sp/min]
Time [days]
Time [ms]
G
Wave shape:
Unchanged
Changed
Amp.
Time [ms]
C.C.
Amp.
Time [hours]
H
A-syn total
A-syn changed waveshape
BSA total
BSA changed waveshape
Neurons that stopped firing
Time [days]

Fig 4. Exogenous hαS decreases neuronal activity and synchronicity of neuronal action potential firing pattern. Rat primary cortical cells were cultured for three weeks and subsequently exposed to either 100 μM hαS or BSA. Neuronal activity was recorded using microelectrode arrays. A) An example of baseline neuronal activity. On the vertical axis, all 60 electrodes are indicated and each tick in the corresponding row represents an action potential. During baseline recordings, started 30 minutes before hαS administration, on average around 50 of the 60 electrodes were active and all activity patterns included network bursts (synchronous firing at all or most electrodes, visualized as 'vertical columns'). B) Recording of the same network four days post hαS administration. C-D) The average number of active electrodes and Array wide firing rate (AWFR; the summed activity of all electrodes in one hour time bins, divided by the bin length) were registered for eight days from eight αS treated cultures (blue) and three BSA (red) [95] treated cultures. E) Neuronal synchronicity slightly increased for two days and then decreased, as indicated by the development of the burstiness index. BSA treated cultures initially showed a similar pattern but here the burstiness recovered after four days F) The action potential shapes and the activity (dots; inset) of a representative neuron at different timepoints (color shift; day 0 = blue, day 7 = red) after addition of αS. G) Examples of neurons with unchanged and changed wave shapes. Top row, overlay of action potentials from every hour color coded as in F. Middle row, correlation coefficients at every hour. Bottom row, action potential amplitudes at every hour. Note the drop in correlation coefficient and amplitude in the last hours in right versus left panel. H) Cumulative histogram showing the fraction of all neurons, with reproducible baseline action potential shape (n = 115), that became inactive in time. Blue indicates all neurons, red shows the fraction of neurons for which the action potential shape changed before becoming inactive. C-E: Error bars represent SEM; n = 8 independent experiments.

https://doi.org/10.1371/journal.pone.0193763.g004

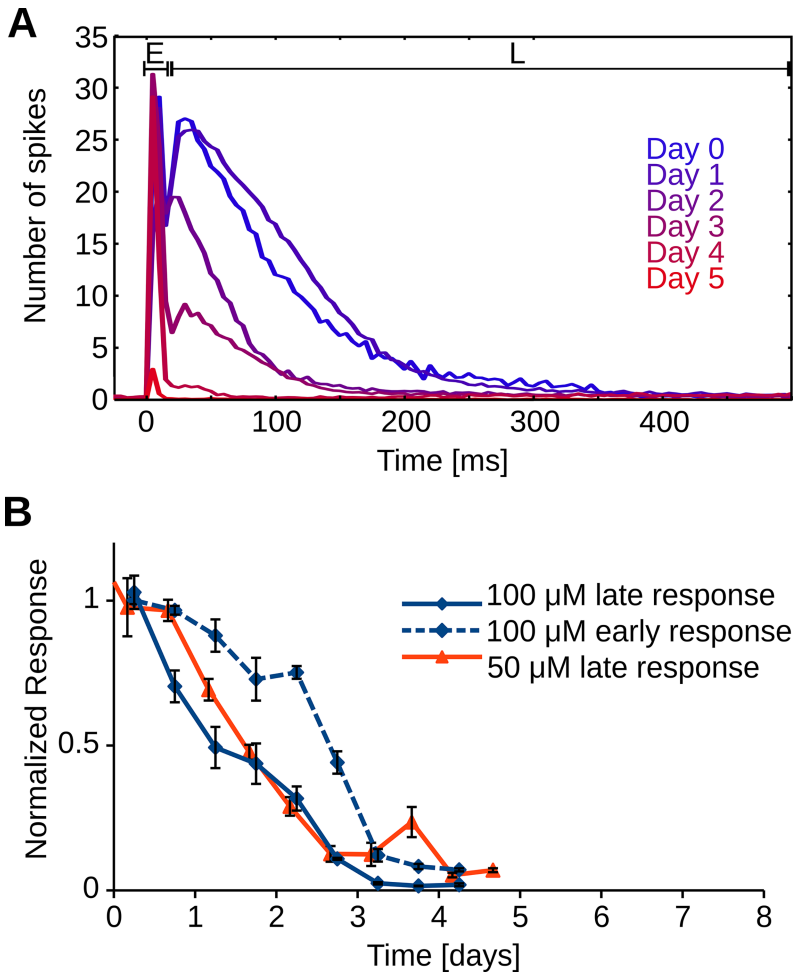

Fig 5. hαS interferes with intercellular communication. Networks of primary cortical rat neurons are electrically stimulated before (day 0) and after administration of 100 μM hαS. A) The first 15 milliseconds after stimulation are dominated by action potentials that were directly triggered by the stimulus pulse (early response; E). These early action potentials are then synaptically propagated through the network and neurons at other electrodes respond up to 300 milliseconds after the stimulation (late response; L). Time progress is visualized by shifting color from blue (day 0) to red (day 5), every line represents the averaged result of 12 stimulation periods (600 stimulations). B) Average development of early and late response after addition of 50 or 100 μM αS, normalized to baseline values. C) Average activity for neural networks treated with 50 μM αS. n = 9 electrodes in three different preparations for each condition.

https://doi.org/10.1371/journal.pone.0193763.g005

Discussion

Cascade of events

Within six hours after the administration of monomeric hαS to mature neural networks derived from rat cortical cells, we observed uptake of fluorescently labeled hαS. Although possible mechanisms on how extracellular proteins can enter the cytoplasm have been proposed, the exact mechanism remains unclear [73]. Between 24 to 48 hours after hαS addition, network excitability started to decrease, as demonstrated by the vanishing synaptically mediated phase of the responses to electrical stimulation. Network excitability may be defined as the average network response to a small stimulus, and thus covers neuronal excitability and synaptic efficacy. Network synchronicity (burstiness) also dropped, confirming the decreasing network excitability. Two days after hαS administration, network excitability dropped to almost zero, but individual neurons were still intact and functioning as demonstrated by the remaining high number of active electrodes, of which action potential shapes and amplitudes were unaffected. At that time, the increase in intracellular hαS concentration resulting from uptake of monomeric protein had resulted in the formation of αS deposits in only a few cells. It generally took five days before one third of the cells contained at least one deposit. Electrophysiological changes, reflected by a decrease in the number of active electrodes, were observed much earlier, between three and four days after αS administration. This decrease in the number of active electrodes might suggest that cells became fully dysfunctional and died. However, cell death and metabolic assays did not support this, leaving the conclusion that the number of active electrodes probably decreased because of decreased network excitability (**Fig 4D**). Thus, network excitability significantly dropped long before LB like deposits became visible. The time line of the events observed in this study are summarized in **Fig 6.** It seems unlikely that the effect on network excitability and the consequent drop in network activity result from the presence of large intracellular αS deposits. The relatively late formation of inclusion bodies is in agreement with a study by Volpicelli et al [11], who saw first inclusion bodies four days post addition of preformed fibrils.

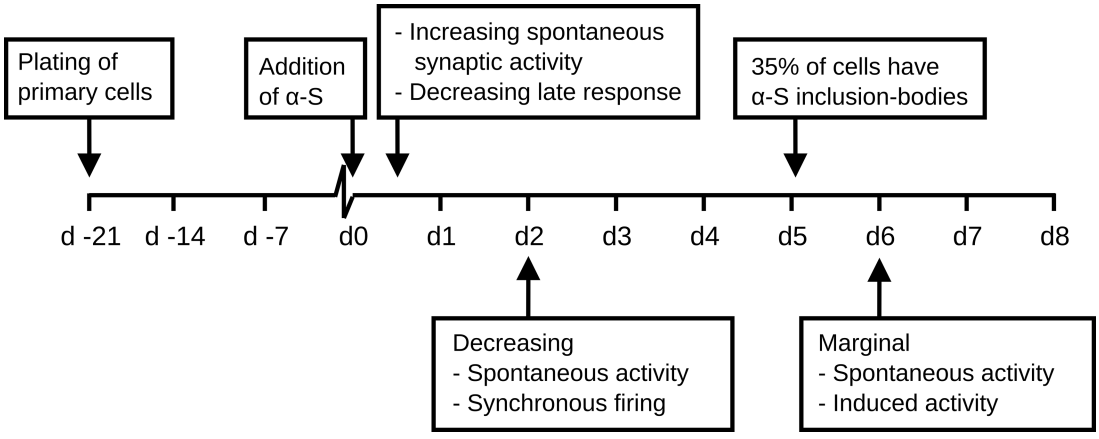

Fig 6. Timeline of events. Three weeks after plating, when neural networks were considered mature, cortical cell cultures were treated with 100 μM αS. Within the first day after αS addition spontaneous synaptic activity rose while electrically induced network response started to decrease. Within two days after addition, spontaneous activity and the number of electrodes on which activity was recorded dropped below baseline. At day five, on average, about one third of the cells had an inclusion body. By day six hardly any spontaneous activity could be recorded and electrical stimulation was no longer able to evoke a network response.

https://doi.org/10.1371/journal.pone.0193763.g006

Interference with network functioning

The decrease in activity might result from neuronal dysfunction, increased inhibition, or from massive synaptic failure. Although a decrease in network activity and failure of isolated synapses in neuronal cultures treated with αS have been reported before [11, 12] we, for the first time, show directly and in a large number of neurons, that impairment of network excitability after addition of αS occurs *before* neuronal degradation. The fact that we were able to stimulate cells directly while spontaneous activity was reduced significantly and action potential shapes and amplitudes remained unaltered, supports the view that reduced activity is not due to neuronal dysfunction. Interference of αS with specific non-synaptic ion channels in the neuronal membrane [74] would alter wave shapes, as would other mechanisms that involve changes in membrane conductance [75–79] or cell death [80]. Alternatively, decreasing activity might be caused by activation of inhibitory receptors. If αS acts as a GABA agonist, we would expect an immediate drop in neural activity upon αS administration. During the first 24 hours, however, the total firing rate increased, while the network response to electrical stimulation already decreased. Therefore, it is unlikely that the eventual decrease in activity was due to increased inhibition. Thus, we conclude that the activity decrease is most likely caused by massive synaptic failure.

Interference with synaptic functioning

Failure of synaptic transmission can take place at many different locations within the signaling cascade. It has been reported that extracellular αS can block post-synaptic receptors directly [81, 82]. At the cytosolic side of the post-synaptic membrane intracellular αS has been reported to enhance internalization of NMDA receptors within 60 minutes [83]. One might speculate that extracellular αS possibly sequesters neurotransmitter within the synaptic cleft, but experimental evidence to support this view is lacking. Monomeric αS or small αS oligomers in the medium might be responsible for such a mechanism, but it is highly unlikely that the intracellular αS deposits are involved.

Alternatively, the excess αS or oligomeric αS aggregates may interfere at the presynaptic side, e.g. in synaptic vesicle trafficking [16, 17] or the synaptic vesicle cycle [18]. Although oligomers may play a role in these mechanisms [63], it is improbable that large αS deposits are responsible; synaptic failure occurs well before large scale cell death. Our analysis confirms that synaptic dysfunction is responsible for synaptic failure, but our data does not allow further differentiation between the above mentioned pre- or post-synaptic mechanisms. Characterization of network activity in the presence of BSA showed that synaptic failure is not a generic effect of surplus protein.

Initial activity increase

The underlying mechanism of the unexpected but robust initial activity increase remains unclear. αS oligomers have been shown to increase the frequency of synaptic transmission due to their pore forming properties [84]. Pro-inflammatory cytokines have been reported also to lead to increased neuronal activity and may decrease firing synchronicity [85–88]. Although we have not characterized our cultures for the presence of microglia [89, 90], this may have caused the observed activity increase. Interesting in this respect is that we do see increased, usually uncorrelated activity as well in early stages of bacterial infection of cultures (personal observation GH & JlF).

Concentration, aggregation and timespan of changes

Recent studies attributed different effects to specific different αS fibril species [12, 91]. In other studies the time required to adjust firing patterns of neurons in response to the addition of

'fibril species was longer [11, 12] than the timespan of activity changes seen in response to the addition of extracellular protein observed here. This slower response may reflect the lower αS concentration used in those studies, up to 1 μM in extracellular assemblies. To mimic the maximal possible effect, we used 50–100 μM, a concentration equivalent to intracellular αS concentrations observed in rat neurons (Fig 2A) and reported in PD and LBD brains [14, 29, 30].

We show that an increased extracellular αS concentration may induce pathology. Though it does not immediately result in cell death, neurons become isolated and network activity drops dramatically. The rapid effect of exogenous αS on the synaptically mediated phase of stimulus responses (within one day), suggests that it can be assigned to the presence of monomers or small oligomers.

Toxicity

The addition of 100 μM hαS monomers had no noteworthy effect on cell viability or metabolic activity on the time scales studied. In agreement with [92] the cytotoxic effects of αS exposure are only small in primary cultures during the first weeks after exposure. The absence of a severe cytotoxic effect (as in SH-SY5Y [37]) might be due to the presence of glial cells, which generally fulfill a supporting function in neuronal networks. Suppressed synaptic functioning, however, generally leads to decreased neuronal activity. Reliable synaptic transmission is essential for regular calcium entry in postsynaptic neurons, which is needed for neuronal survival [93, 94] and the remaining activity may be insufficient for long-term neuronal survival. It remains to be seen whether this discrepancy between cell death and loss of synaptic transmission can also be observed in neurons derived from other parts of the nervous system and whether the same mechanism is present and crucial in the etiology of synucleopathies in patients.

Conclusion

Combined, these data support the idea that synaptic failure is the primary effect induced by high concentration of αS. Decreasing activity results from synaptic failure rather than neuronal dysfunction. Neuronal death in our study may have occurred secondary to synaptic failure due to insufficient remaining activity. This mechanism suggests that local high concentrations of monomeric αS or perhaps small oligomeric αS species might play an important role in synucleopathies.

Acknowledgments

This project was funded in part from NWO-CW VIDI grant number (700.59.423) to M.C and in part by a MIRA voucher to JlF and MC. We further want to thank K. van Leijenhorst-Groener and I. Konings for excellent technical assistance.

Author Contributions

Conceptualization: V. Subramaniam, J. le Feber, M. M. A. E. Claessens.

Formal analysis: G. C. Hassink, C. C. Raiss, I. M. J. Segers-Nolten, J. le Feber, M. M. A. E. Claessens.

Funding acquisition: J. le Feber, M. M. A. E. Claessens.

Investigation: G. C. Hassink, C. C. Raiss, I. M. J. Segers-Nolten, J. le Feber.

Methodology: J. le Feber, M. M. A. E. Claessens.

Resources: R. J. A. van Wezel.

Software: G. C. Hassink, J. le Feber.

Supervision: J. le Feber, M. M. A. E. Claessens.

Visualization: I. M. J. Segers-Nolten.

Writing – original draft: G. C. Hassink, C. C. Raiss, J. le Feber, M. M. A. E. Claessens.

Writing – review & editing: G. C. Hassink, R. J. A. van Wezel, V. Subramaniam, J. le Feber, M. M. A. E. Claessens.

References

1. Spillantini MG, Goedert M. The alpha-synucleinopathies: Parkinson's disease, dementia with Lewy bodies, and multiple system atrophy. Annals of the New York Academy of Sciences. 2000; 920:16–27. WOS:000171939600003. PMID: 11193145
2. Jellinger KA. Neuropathological spectrum of synucleinopathies. Movement Disorders. 2003; 18:S2–S12. https://doi.org/10.1002/mds.10557 WOS:000185514400002. PMID: 14502650
3. Schulz-Schaeffer W. Is Cell Death Primary or Secondary in the Pathophysiology of Idiopathic Parkinson's Disease? Biomolecules. 2015; 5(3):1467–79. https://doi.org/10.3390/biom5031467 Schulz-Schaeffer2015. PMID: 26193328
4. Lee HJ, Patel S, Lee SJ. Intravesicular localization and exocytosis of alpha-synuclein and its aggregates. J Neurosci. 2005; 25(25):6016–24. https://doi.org/10.1523/JNEUROSCI.0692-05.2005 PMID: 15976091.
5. Fortin DL, Nemani VM, Voglmaier SM, Anthony MD, Ryan TA, Edwards RH. Neural activity controls the synaptic accumulation of alpha-synuclein. Journal of Neuroscience. 2005; 25(47):10913–21. https://doi.org/10.1523/JNEUROSCI.2922-05.2005 WOS:000233460400012. PMID: 16306404
6. Lee SJ, Desplats P, Lee HJ, Bae EJ, Patrick C, Rockenstein E, et al. Inclusion Formation and Neuronal Cell Death through Neuron-to-Neuron Transmission of Alpha-Synuclein. Journal of neurochemistry. 2009; 110:137-. WOS:000268550400380.
7. Danzer KM, Ruf WP, Putcha P, Joyner D, Hashimoto T, Glabe C, et al. Heat-shock protein 70 modulates toxic extracellular alpha-synuclein oligomers and rescues trans-synaptic toxicity. FASEB J. 2011; 25(1):326–36. https://doi.org/10.1096/fj.10-164624 PMID: 20876215; PubMed Central PMCID: PMC3005424.
8. Hansen C, Angot E, Bergstrom AL, Steiner JA, Pieri L, Paul G, et al. alpha-Synuclein propagates from mouse brain to grafted dopaminergic neurons and seeds aggregation in cultured human cells. J Clin Invest. 2011; 121(2):715–25. https://doi.org/10.1172/JCI43366 PMID: 21245577; PubMed Central PMCID: PMC3026723.
9. Kordower JH, Chu Y, Hauser RA, Freeman TB, Olanow CW. Lewy body-like pathology in long-term embryonic nigral transplants in Parkinson's disease. Nat Med. 2008; 14(5):504–6. https://doi.org/10.1038/nm1747 PMID: 18391962.
10. Li JY, Englund E, Holton JL, Soulet D, Hagell P, Lees AJ, et al. Lewy bodies in grafted neurons in subjects with Parkinson's disease suggest host-to-graft disease propagation. Nat Med. 2008; 14(5):501–3. https://doi.org/10.1038/nm1746 PMID: 18391963.
11. Volpicelli-Daley LA, Luk KC, Patel TP, Tanik SA, Riddle DM, Stieber A, et al. Exogenous alpha-synuclein fibrils induce Lewy body pathology leading to synaptic dysfunction and neuron death. Neuron. 2011; 72(1):57–71. https://doi.org/10.1016/j.neuron.2011.08.033 PMID: 21982369; PubMed Central PMCID: PMC3204802.
12. Peelaerts W, Bousset L, Van der Perren A, Moskalyuk A, Pulizzi R, Giugliano M, et al. alpha-Synuclein strains cause distinct synucleinopathies after local and systemic administration. Nature. 2015; 522 (7556):340–4. https://doi.org/10.1038/nature14547 PMID: 26061766.
13. Maroteaux L, Campanelli JT, Scheller RH. Synuclein: a neuron-specific protein localized to the nucleus and presynaptic nerve terminal. J Neurosci. 1988; 8(8):2804–15. PMID: 3411354.
14. Iwai A, Masliah E, Yoshimoto M, Ge NF, Flanagan L, Desilva HAR, et al. The Precursor Protein of Non-a-Beta Component of Alzheimers-Disease Amyloid Is a Presynaptic Protein of the Central-Nervous-System. Neuron. 1995; 14(2):467–75. https://doi.org/10.1016/0896-6273(95)90302-X WOS: A1995QH29400024. PMID: 7857654
15. Fortin DL, Troyer MD, Nakamura K, Kubo S, Anthony MD, Edwards RH. Lipid rafts mediate the synaptic localization of alpha-synuclein. J Neurosci. 2004; 24(30):6715–23. https://doi.org/10.1523/JNEUROSCI.1594-04.2004 PMID: 15282274.

16. Nemani VM, Lu W, Berge V, Nakamura K, Onoa B, Lee MK, et al. Increased Expression of alpha-Synuclein Reduces Neurotransmitter Release by Inhibiting Synaptic Vesicle Reclustering after Endocytosis. Neuron. 2010; 65(1):66–79. https://doi.org/10.1016/j.neuron.2009.12.023 WOS:000273791200009. PMID: 20152114

17. Scott DA, Tabarean I, Tang Y, Cartier A, Masliah E, Roy S. A pathologic cascade leading to synaptic dysfunction in alpha-synuclein-induced neurodegeneration. J Neurosci. 2010; 30(24):8083–95. https://doi.org/10.1523/JNEUROSCI.1091-10.2010 PMID: 20554859; PubMed Central PMCID: PMC2901533.

18. Busch DJ, Oliphint PA, Walsh RB, Banks SM, Woods WS, George JM, et al. Acute increase of alpha-synuclein inhibits synaptic vesicle recycling evoked during intense stimulation. Mol Biol Cell. 2014; 25 (24):3926–41. https://doi.org/10.1091/mbc.E14-02-0708 PMID: 25273557; PubMed Central PMCID: PMCPMC4244201.

19. Chandra S, Fornai F, Kwon HB, Yazdani U, Atasoy D, Liu XR, et al. Double-knockout mice for alpha- and beta-synucleins: Effect on synaptic functions. Proceedings of the National Academy of Sciences of the United States of America. 2004; 101(41):14966–71. https://doi.org/10.1073/pnas.0406283101 WOS:000224488000051. PMID: 15465911

20. Chandra S, Gallardo G, Fernandez-Chacon R, Schluter OM, Sudhof TC. alpha-synuclein cooperates with CSP alpha in preventing neurodegeneration. Cell. 2005; 123(3):383–96. https://doi.org/10.1016/j.cell.2005.09.028 WOS:000233264300008. PMID: 16269331

21. Umbach JA, Zinsmaier KE, Eberle KK, Buchner E, Benzer S, Gundersen CB. Presynaptic dysfunction in Drosophila csp mutants. Neuron. 1994; 13(4):899–907. PMID: 7946336.

22. Zinsmaier KE, Eberle KK, Buchner E, Walter N, Benzer S. Paralysis and early death in cysteine string protein mutants of Drosophila. Science. 1994; 263(5149):977–80. PMID: 8310297.

23. Schaab C, Geiger T, Stoehr G, Cox J, Mann M. Analysis of high accuracy, quantitative proteomics data in the MaxQB database. Molecular \& cellular proteomics: MCP. 2012; 11(3):M111.014068. https://doi.org/10.1074/mcp.M111.014068 Schaab2012. PMID: 22301388

24. Genecards. http://www.genecards.org/cgi-bin/carddisp.pl?gene=SNCA&keywords=alpha,synuclein.

25. Zeskind BJ, Jordan CD, Timp W, Trapani L, Waller G, Horodincu V, et al. Nucleic acid and protein mass mapping by live-cell deep-ultraviolet microscopy. Nat Methods. 2007; 4(7):567–9. https://doi.org/10.1038/nmeth1053 PMID: 17546037.

26. Wilhelm BG, Mandad S, Truckenbrodt S, Krhnert K, Schfer C, Rammner B, et al. Vesicle Trafficking Proteins. 2014; 344(6187):1023–8.

27. Fagan ES, Pihlstrom L. Genetic risk factors for cognitive decline in Parkinson's disease: a review of the literature. Eur J Neurol. 2017; 24(4):561–e20. https://doi.org/10.1111/ene.13258 PMID: 28220571.

28. Klein C, Westenberger A. Genetics of Parkinson's Disease. Cold Spring Harbor Perspectives in Medicine. 2012; 2(1). ARTN a008888 10.1101/cshperspect.a008888. WOS:000314239200007.

29. Chu Y, Kordower JH. Age-associated increases of alpha-synuclein in monkeys and humans are associated with nigrostriatal dopamine depletion: Is this the target for Parkinson's disease? Neurobiology of disease. 2007; 25(1):134–49. https://doi.org/10.1016/j.nbd.2006.08.021 Chu2007. PMID: 17055279

30. Brudek T, Winge Ka. Altered Alpha-Synuclein, Parkin, and Synphilin Isoform Levels in Multiple System Atrophy Brains. Journal of neurochemistry. 2015:n/a—n/a. https://doi.org/10.1111/jnc.13392 Brudek2015. PMID: 26465922

31. Klucken J, Ingelsson M, Shin Y, Irizarry MC, Hedley-Whyte ET, Frosch M, et al. Clinical and biochemical correlates of insoluble alpha-synuclein in dementia with Lewy bodies. Acta Neuropathol. 2006; 111 (2):101–8. https://doi.org/10.1007/s00401-005-0027-7 PMID: 16482476.

32. Yin J, Han J, Zhang C, Ma QL, Li X, Cheng F, et al. C-terminal part of alpha-synuclein mediates its activity in promoting proliferation of dopaminergic cells. J Neural Transm (Vienna). 2011; 118(8):1155–64. https://doi.org/10.1007/s00702-011-0592-y PMID: 21331461.

33. Mollenhauer B, Cullen V, Kahn I, Krastins B, Outeiro TF, Pepivani I, et al. Direct quantification of CSF alpha-synuclein by ELISA and first cross-sectional study in patients with neurodegeneration. Experimental neurology. 2008; 213(2):315–25. https://doi.org/10.1016/j.expneurol.2008.06.004 Mollenhauer2008. PMID: 18625222

34. Allen C, Thornton P, Denes A, McColl BW, Pierozynski A, Monestier M, et al. Neutrophil cerebrovascular transmigration triggers rapid neurotoxicity through release of proteases associated with decondensed DNA. J Immunol. 2012; 189(1):381–92. https://doi.org/10.4049/jimmunol.1200409 PMID: 22661091; PubMed Central PMCID: PMCPMC3381844.

35. Rodriguez-Grande B, Blackabey V, Gittens B, Pinteaux E, Denes A. Loss of substance P and inflammation precede delayed neurodegeneration in the substantia nigra after cerebral ischemia. Brain Behav Immun. 2013; 29:51–61. https://doi.org/10.1016/j.bbi.2012.11.017 PMID: 23232501.

36. Kim S, Cho SH, Kim KY, Shin KY, Kim HS, Park CH, et al. Alpha-synuclein induces migration of BV-2 microglial cells by up-regulation of CD44 and MT1-MMP. Journal of neurochemistry. 2009; 109 (5):1483–96. https://doi.org/10.1111/j.1471-4159.2009.06075.x PMID: 19457162.

37. Raiss CC, Braun TS, Konings IB, Grabmayr H, Hassink GC, Sidhu A, et al. Functionally different alpha-synuclein inclusions yield insight into Parkinson's disease pathology. Sci Rep. 2016; 6:23116. https://doi.org/10.1038/srep23116 PMID: 26984067; PubMed Central PMCID: PMCPMC4794800.

38. Shi M, Liu C, Cook TJ, Bullock KM, Zhao Y, Ginghina C, et al. Plasma exosomal alpha-synuclein is likely CNS-derived and increased in Parkinson's disease. Acta Neuropathol. 2014. https://doi.org/10.1007/s00401-014-1314-y PMID: 24997849.

39. Chistiakov DA, Chistiakov AA. alpha-Synuclein-carrying extracellular vesicles in Parkinson's disease: deadly transmitters. Acta Neurol Belg. 2016. https://doi.org/10.1007/s13760-016-0679-1 PMID: 27473175.

40. Bonneh-Barkay D, Wiley CA. Brain extracellular matrix in neurodegeneration. Brain Pathol. 2009; 19 (4):573–85. https://doi.org/10.1111/j.1750-3639.2008.00195.x PMID: 18662234; PubMed Central PMCID: PMCPMC2742568.

41. Kurtz A, Oh SJ. Age related changes of the extracellular matrix and stem cell maintenance. Prev Med. 2012;54 Suppl:S50–6. https://doi.org/10.1016/j.ypmed.2012.01.003 PMID: 22285947.

42. Morawski M, Filippov M, Tzinia A, Tsilibary E, Vargova L. ECM in brain aging and dementia. Prog Brain Res. 2014; 214:207–27. https://doi.org/10.1016/B978-0-444-63486-3.00010-4 PMID: 25410360.

43. Lepelletier FX, Mann DM, Robinson AC, Pinteaux E, Boutin H. Early changes in extracellular matrix in Alzheimer's disease. Neuropathol Appl Neurobiol. 2015. https://doi.org/10.1111/nan.12295 PMID: 26544797.

44. Kaganovich D, Kopito R, Frydman J. Misfolded proteins partition between two distinct quality control compartments. Nature. 2008; 454(7208):1088–95. https://doi.org/10.1038/nature07195 PMID: 18756251; PubMed Central PMCID: PMC2746971.

45. Semerdzhiev SA, Dekker DR, Subramaniam V, Claessens MM. Self-assembly of protein fibrils into suprafibrillar aggregates: bridging the nano- and mesoscale. ACS Nano. 2014; 8(6):5543–51. https://doi.org/10.1021/nn406309c PMID: 24805840.

46. van Raaij ME, Segers-Nolten IM, Subramaniam V. Quantitative morphological analysis reveals ultrastructural diversity of amyloid fibrils from alpha-synuclein mutants. Biophys J. 2006; 91(11):L96–8. https://doi.org/10.1529/biophysj.106.090449 PMID: 16997873; PubMed Central PMCID: PMC1635669.

47. van Rooijen BD, Claessens MM, Subramaniam V. Lipid bilayer disruption by oligomeric alpha-synuclein depends on bilayer charge and accessibility of the hydrophobic core. Biochim Biophys Acta. 2009; 1788 (6):1271–8. https://doi.org/10.1016/j.bbamem.2009.03.010 PMID: 19328772.

48. Kaylor J, Bodner N, Edridge S, Yamin G, Hong DP, Fink AL. Characterization of oligomeric intermediates in alpha-synuclein fibrillation: FRET studies of Y125W/Y133F/Y136F alpha-synuclein. J Mol Biol. 2005; 353(2):357–72. https://doi.org/10.1016/j.jmb.2005.08.046 PMID: 16171820.

49. Stegenga J, Le Feber J, Marani E, Rutten WL. The effect of learning on bursting. IEEE Trans Biomed Eng. 2009; 56(4):1220–7. https://doi.org/10.1109/TBME.2008.2006856 PMID: 19272893.

50. Romijn HJ, van Huizen F, Wolters PS. Towards an improved serum-free, chemically defined medium for long-term culturing of cerebral cortex tissue. Neurosci Biobehav Rev. 1984; 8(3):301–34. PMID: 6504415.

51. Gold C, Henze DA, Koch C, Buzsaki G. On the origin of the extracellular action potential waveform: A modeling study. Journal of neurophysiology. 2006; 95(5):3113–28. https://doi.org/10.1152/jn.00979.2005 WOS:000236797100035. PMID: 16467426

52. van Pelt J, Wolters PS, Corner MA, Rutten WLC, Ramakers GJA. Long-term characterization of firing dynamics of spontaneous bursts in cultured neural networks. Ieee Transactions on Biomedical Engineering. 2004; 51(11):2051–62. https://doi.org/10.1109/TBME.2004.827936 WOS:000224657100020. PMID: 15536907

53. Wagenaar D, DeMarse TB, Potter SM. MeaBench: A toolset for multi-electrode data acquisition and online analysis. 2005 2nd Internatinoal Ieee/Embs Conference on Neural Engineering. 2005:518–21. WOS:000229610400138.

54. Akanda N, Molnar P, Stancescu M, Hickman JJ. Analysis of toxin-induced changes in action potential shape for drug development. J Biomol Screen. 2009; 14(10):1228–35. https://doi.org/10.1177/1087057109348378 PMID: 19801532; PubMed Central PMCID: PMCPMC3829631.

55. Law JK, Yeung CK, Hofmann B, Ingebrandt S, Rudd JA, Offenhausser A, et al. The use of microelectrode array (MEA) to study the protective effects of potassium channel openers on metabolically

compromised HL-1 cardiomyocytes. Physiol Meas. 2009; 30(2):155–67. https://doi.org/10.1088/0967-3334/30/2/004 PMID: 19136734.

56. le Feber J, Tzafi Pavlidou S, Erkamp N, van Putten MJ, Hofmeijer J. Progression of Neuronal Damage in an In Vitro Model of the Ischemic Penumbra. PLoS One. 2016; 11(2):e0147231. https://doi.org/10.1371/journal.pone.0147231 PMID: 26871437; PubMed Central PMCID: PMCPMC4752264.

57. Wagenaar DA, Madhavan R, Pine J, Potter SM. Controlling bursting in cortical cultures with closed-loop multi-electrode stimulation. Journal of Neuroscience. 2005; 25(3):680–8. https://doi.org/10.1523/JNEUROSCI.4209-04.2005 WOS:000226414700017. PMID: 15659605

58. Hofmeijer J, Mulder AT, Farinha AC, van Putten MJ, le Feber J. Mild hypoxia affects synaptic connectivity in cultured neuronal networks. Brain Res. 2014; 1557:180–9. https://doi.org/10.1016/j.brainres.2014.02.027 PMID: 24560899.

59. Shahaf G, Marom S. Learning in networks of cortical neurons. Journal of Neuroscience. 2001; 21 (22):8782–8. WOS:000172012700012. PMID: 11698590

60. Bakkum DJ, Chao ZC, Potter SM. Long-term activity-dependent plasticity of action potential propagation delay and amplitude in cortical networks. PloS one. 2008; 3(5):e2088. https://doi.org/10.1371/journal.pone.0002088 Bakkum2008. PMID: 18461127

61. Reinartz S, Biro I, Gal A, Giugliano M, Marom S. Synaptic dynamics contribute to long-term single neuron response fluctuations. Front Neural Circuits. 2014; 8:71. https://doi.org/10.3389/fncir.2014.00071 PMID: 25071452; PubMed Central PMCID: PMC4077315.

62. Fedorovich S, Hofmeijer J, van Putten MJ, le Feber J. Reduced Synaptic Vesicle Recycling during Hypoxia in Cultured Cortical Neurons. Front Cell Neurosci. 2017; 11:32. https://doi.org/10.3389/fncel.2017.00032 PMID: 28261063; PubMed Central PMCID: PMCPMC5311063.

63. Stefanovic AN, Lindhoud S, Semerdzhiev SA, Claessens MM, Subramaniam V. Oligomers of Parkinson's Disease-Related alpha-Synuclein Mutants Have Similar Structures but Distinctive Membrane Permeabilization Properties. Biochemistry. 2015; 54(20):3142–50. https://doi.org/10.1021/bi501369k PMID: 25909158.

64. Zhou W, Hurlbert MS, Schaack J, Prasad KN, Freed CR. Overexpression of human alpha-synuclein causes dopamine neuron death in rat primary culture and immortalized mesencephalon-derived cells. Brain Res. 2000; 866(1–2):33–43. PMID: 10825478.

65. Stefanova N, Klimaschewski L, Poewe W, Wenning GK, Reindl M. Glial cell death induced by overexpression of alpha-synuclein. Journal of Neuroscience Research. 2001; 65(5):432–8. https://doi.org/10.1002/jnr.1171 WOS:000170734500010. PMID: 11536327

66. Zhou WB, Schaack J, Zawada WM, Freed CR. Overexpression of human alpha-synuclein causes dopamine neuron death in primary human mesencephalic culture. Brain Research. 2002; 926(1–2):42–50. Pii S0006-8993(01)03292-9 https://doi.org/10.1016/S0006-8993(01)03292-9 WOS:000173904000006. PMID: 11814405

67. Prasad JE, Kumar B, Andreatta C, Nahreini P, Hanson AJ, Yan XD, et al. Overexpression of alpha-synuclein decreased viability and enhanced sensitivity to prostaglandin E-2, hydrogen peroxide, and a nitric oxide donor in differentiated neuroblastoma cells. Journal of Neuroscience Research. 2004; 76 (3):415–22. https://doi.org/10.1002/jnr.20058 WOS:000221183100016. PMID: 15079871

68. Lee SJ. Origins and effects of extracellular alpha-synuclein: Implications in Parkinson's disease. Journal of Molecular Neuroscience. 2008; 34(1):17–22. https://doi.org/10.1007/s12031-007-0012-9 WOS:000251866900003. PMID: 18157654

69. Desplats P, Lee HJ, Bae EJ, Patrick C, Rockenstein E, Crews L, et al. Inclusion formation and neuronal cell death through neuron-to-neuron transmission of alpha-synuclein. Proc Natl Acad Sci U S A. 2009; 106(31):13010–5. https://doi.org/10.1073/pnas.0903691106 PMID: 19651612; PubMed Central PMCID: PMC2722313.

70. Lu L, Yang H. OVEREXPRESSION OF alpha-SYNUCLEIN GENE CAUSED DOPAMINERGIC NEURON DAMAGE IN SUBSTANTIA NIGRA OF RATS. Journal of neurochemistry. 2009; 110:195-. WOS:000268550400532.

71. Lee S-J, Lim H-S, Masliah E, Lee H-J. Protein aggregate spreading in neurodegenerative diseases: problems and perspectives. Neuroscience research. 2011; 70(4):339–48. https://doi.org/10.1016/j.neures.2011.05.008 Lee2011. PMID: 21624403

72. Luk KC, Kehm V, Carroll J, Zhang B, O'Brien P, Trojanowski JQ, et al. Pathological alpha-synuclein transmission initiates Parkinson-like neurodegeneration in nontransgenic mice. Science. 2012; 338 (6109):949–53. https://doi.org/10.1126/science.1227157 PMID: 23161999; PubMed Central PMCID: PMC3552321.

73. Lee HJ, Bae EJ, Lee SJ. Extracellular alpha-synuclein-a novel and crucial factor in Lewy body diseases. Nature Reviews Neurology. 2014; 10(2):92–8. https://doi.org/10.1038/nrneurol.2013.275 WOS:000331061200009. PMID: 24468877

74. Thomas MP, Chartrand K, Reynolds A, Vitvitsky V, Banerjee R, Gendelman HE. Ion channel blockade attenuates aggregated alpha synuclein induction of microglial reactive oxygen species: relevance for the pathogenesis of Parkinson's disease. Journal of neurochemistry. 2007; 100(2):503–19. https://doi.org/10.1111/j.1471-4159.2006.04315.x WOS:000242993300021. PMID: 17241161

75. Adamczyk A, Strosznajder JB. Alpha-synuclein potentiates Ca2+ influx through voltage-dependent Ca2+ channels. Neuroreport. 2006; 17(18):1883–6. https://doi.org/10.1097/WNR.0b013e3280115185 WOS:000243538600010. PMID: 17179863

76. Furukawa K, Matsuzaki-Kobayashi M, Hasegawa T, Kikuchi A, Sugeno N, Itoyama Y, et al. Plasma membrane ion permeability induced by mutant alpha-synuclein contributes to the degeneration of neural cells. Journal of neurochemistry. 2006; 97(4):1071–7. https://doi.org/10.1111/j.1471-4159.2006.03803.x WOS:000237063200016. PMID: 16606366

77. Feng LR, Federoff HJ, Vicini S, Maguire-Zeiss KA. alpha-Synuclein mediates alterations in membrane conductance: a potential role for alpha-synuclein oligomers in cell vulnerability. European Journal of Neuroscience. 2010; 32(1):10–7. https://doi.org/10.1111/j.1460-9568.2010.07266.x WOS:000279612400002. PMID: 20550572

78. Geng XH, Lou HY, Wang JA, Li LH, Swanson AL, Sun M, et al. alpha-Synuclein binds the K-ATP channel at insulin-secretory granules and inhibits insulin secretion. American Journal of Physiology-Endocrinology and Metabolism. 2011; 300(2):E276–E86. https://doi.org/10.1152/ajpendo.00262.2010 WOS:000289011600003. PMID: 20858756

79. Mironov SL. alpha-Synuclein forms non-selective cation channels and stimulates ATP-sensitive potassium channels in hippocampal neurons. J Physiol. 2014. https://doi.org/10.1113/jphysiol.2014.280974 PMID: 25326450.

80. Adamczyk A, Kamierczak A, Czapski GA, Strosznajder JB. Alpha-synuclein induced cell death in mouse hippocampal (HT22) cells is mediated by nitric oxide-dependent activation of caspase-3. FEBS letters. 2010; 584(15):3504–8. https://doi.org/10.1016/j.febslet.2010.07.019 Adamczyk2010. PMID: 20638384

81. Huls S, Hogen T, Vassallo N, Danzer KM, Hengerer B, Giese A, et al. AMPA-receptor-mediated excitatory synaptic transmission is enhanced by iron-induced alpha-synuclein oligomers. Journal of neurochemistry. 2011; 117(5):868–78. https://doi.org/10.1111/j.1471-4159.2011.07254.x PMID: 21426349.

82. Liu Q, Emadi S, Shen JX, Sierks MR, Wu J. Human alpha 4 beta 2 Nicotinic Acetylcholine Receptor as a Novel Target of Oligomeric alpha-Synuclein. Plos One. 2013; 8(2). ARTN e55886 10.1371/journal.pone.0055886. WOS:000315184200029.

83. Cheng FR, Li X, Li YH, Wang CD, Wang T, Liu GW, et al. alpha-Synuclein promotes clathrin-mediated NMDA receptor endocytosis and attenuates NMDA-induced dopaminergic cell death. Journal of neurochemistry. 2011; 119(4):815–25. https://doi.org/10.1111/j.1471-4159.2011.07460.x WOS:000297020300014. PMID: 21883224

84. Pacheco CR, Morales CN, Ramirez AE, Munoz FJ, Gallegos SS, Caviedes PA, et al. Extracellular alpha-synuclein alters synaptic transmission in brain neurons by perforating the neuronal plasma membrane. Journal of neurochemistry. 2015; 132(6):731–41. https://doi.org/10.1111/jnc.13060 PMID: 25669123.

85. Barger SW, Basile AS. Activation of microglia by secreted amyloid precursor protein evokes release of glutamate by cystine exchange and attenuates synaptic function. Journal of neurochemistry. 2001; 76(3):846–54. PMID: 11158256.

86. Hadjilambreva G, Mix E, Rolfs A, Muller J, Strauss U. Neuromodulation by a cytokine: Interferon-beta differentially augments neocortical neuronal activity and excitability. Journal of neurophysiology. 2005; 93(2):843–52. https://doi.org/10.1152/jn.01224.2003 WOS:000226342000019. PMID: 15385586

87. Schapansky J, Nardozzi JD, LaVoie MJ. The complex relationships between microglia, alpha-synuclein, and LRRK2 in Parkinson's disease. Neuroscience. 2015; 302:74–88. https://doi.org/10.1016/j.neuroscience.2014.09.049 PMID: 25284317; PubMed Central PMCID: PMCPMC4383729.

88. Iori V, Frigerio F, Vezzani A. Modulation of neuronal excitability by immune mediators in epilepsy. Curr Opin Pharmacol. 2016; 26:118–23. https://doi.org/10.1016/j.coph.2015.11.002 PMID: 26629681; PubMed Central PMCID: PMCPMC4716878.

89. Combs CK, Johnson DE, Karlo JC, Cannady SB, Landreth GE. Inflammatory mechanisms in Alzheimer's disease: inhibition of beta-amyloid-stimulated proinflammatory responses and neurotoxicity by PPARgamma agonists. J Neurosci. 2000; 20(2):558–67. PMID: 10632585.

90. Gresa-Arribas N, Vieitez C, Dentesano G, Serratosa J, Saura J, Sola C. Modelling neuroinflammation in vitro: a tool to test the potential neuroprotective effect of anti-inflammatory agents. PLoS One. 2012; 7(9):e45227. https://doi.org/10.1371/journal.pone.0045227 PMID: 23028862; PubMed Central PMCID: PMCPMC3447933.

91. Bousset L, Pieri L, Ruiz-Arlandis G, Gath J, Jensen PH, Habenstein B, et al. Structural and functional characterization of two alpha-synuclein strains. Nature communications. 2013; 4:2575. https://doi.org/10.1038/ncomms3575 Bousset2013. PMID: 24108358

92. Volpicelli-Daley LA, Luk KC, Lee VMY. Addition of exogenous α-synuclein preformed fibrils to primary neuronal cultures to seed recruitment of endogenous α-synuclein to Lewy body and Lewy neurite–like aggregates. Nat Protocols. 2014; 9(9):2135–46. https://doi.org/10.1038/nprot.2014.143 http://www.nature.com/nprot/journal/v9/n9/abs/nprot.2014.143.html#supplementary-information. PMID: 25122523

93. Ghosh A, Carnahan J, Greenberg ME. Requirement for Bdnf in Activity-Dependent Survival of Cortical-Neurons. Science. 1994; 263(5153):1618–23. https://doi.org/10.1126/science.7907431 WOS: A1994NB67300034. PMID: 7907431

94. Mao ZX, Bonni A, Xia F, Nadal-Vicens M, Greenberg ME. Neuronal activity-dependent cell survival mediated by transcription factor MEF2. Science. 1999; 286(5440):785–90. https://doi.org/10.1126/science.286.5440.785 WOS:000083303200058. PMID: 10531066

95. Spencer CCA, Plagnol V, Strange A, Gardner M, Paisan-Ruiz C, Band G, et al. Dissection of the genetics of Parkinson's disease identifies an additional association 5' of SNCA and multiple associated haplotypes at 17q21. Human Molecular Genetics. 2011; 20(2):345–53. https://doi.org/10.1093/hmg/ddq469 WOS:000285626900013. PMID: 21044948